The Astrophysical Journal, 657:167–176, 2007 March 1

INVESTIGATING THE NUCLEAR OBSCURATION IN TWO TYPES OF SEYFERT 2 GALAXIES

X. W. Shu, J. X. Wang, P. Jiang, L. L. Fan, and T. G. Wang
Center for Astrophysics, University of Science and Technology of China (USTC), Hefei, Anhui, China; Joint Institute for Galaxy and Cosmology, USTC and Shanghai Astronomical Observatory, Chinese Academy of Sciences; jxw@ustc.edu.cn
Received 2006 September 5; accepted 2006 November 2

ABSTRACT

We build a large sample of Seyfert 2 galaxies (Sy2s) with both optical spectropolarimetric and X-ray data available, in which 29 of the Sy2s have a detection of polarized broad emission lines (PBLs) and 25 do not. We find that for luminous Sy2s with $L_{[\mathrm{O\,III}]} > 10^{41}$ ergs s^{-1}, sources with PBLs have smaller X-ray absorption column densities in comparison to those without PBLs (at a 92.3% confidence level): most of the Sy2s with $N_{\mathrm{H}} < 10^{23.8}$ cm^{-2} show PBLs (86%; 12 out of 14), while the fraction is much smaller for sources with heavier obscuration (54%; 15 out of 28). The confidence level of the difference in absorption bounces up to 99.1% when using the thickness ("T") ratio ($F_{2\text{–}10\,\mathrm{keV}}/F_{[\mathrm{O\,III}]}$) as an indicator. We rule out observation or selection bias as the origin for the difference. Our results, for the first time with high statistical confidence, show that, in additional to the activity of the nuclei, the nuclear obscuration also plays an important role in the visibility of PBLs in Sy2s. These results can be interpreted in the framework of the unified model. We can reach these results in the unified model if (1) the absorption column density is higher at large inclinations and (2) the scattering region is obscured at large inclinations.

Subject headings: galaxies: active — galaxies: Seyfert — polarization

1. INTRODUCTION

The active galactic nucleus (AGN) unification model proposes that Seyfert 1 and 2 galaxies (hereafter Sy1s and Sy2s) are intrinsically the same objects, and the absence of broad emission lines in Sy2s is ascribed to the obscuration along the line of sight by a parsec-scale dusty torus (see the review by Antonucci 1993). The most convincing evidence is the detection of polarized broad emission lines (hereafter PBLs) in some Seyfert 2 galaxies (Antonucci & Miller 1985; Tran 1995; Heisler et al. 1997; Moran et al. 2000; Lumsden et al. 2001; Tran 2001). Similarly, infrared (IR) observations showed the existence of obscured broad-line regions (BLRs) in Sy2s (Veilleux et al. 1997). Further evidence supporting the unification model comes from X-ray observations of Sy2s that show large amounts of obscuration, typically above 10^{23} cm^{-2} (e.g., Turner et al. 1997; Bassani et al. 1999).

Despite the fact that the observations do generally support an orientation-based unification model, only ~50% of Sy2s show broad lines in the polarized spectrum (e.g., Tran 2001; Gu & Huang 2002). With an optical spectropolarimetric study of a well-defined and statistically complete *Infrared Astronomical Satellite* (*IRAS*) 60 μm–selected Sy2 sample, Heisler et al. (1997) found a relationship between the detectability of polarized broad Hα and the *IRAS* f_{60}/f_{25} flux ratio, which is that only those galaxies with warm *IRAS* colors ($f_{60}/f_{25} < 4.0$) show PBLs. Heisler et al. suggested that the detectability of PBLs simply depends on the inclination of the torus to the line of sight: in a Sy2 with the torus highly inclined, a cooler infrared color is expected, and the broad-line scattering screen could also be obscured.

A simple prediction of the inclination-related model is that Sy2s without PBLs (hereafter NPBL Sy2s) should show higher absorption column density, since they are more inclined than the Sy2s with PBLs (hereafter PBL Sy2s). However, following studies have claimed that there is no difference in the absorption column density between the two types of Sy2s (Alexander 2001; Tran 2001, 2003). Furthermore, as Alexander (2001; also see Lumsden et al. 2001; Tran 2001, 2003; Gu & Huang 2002) pointed out, the difference in the *IRAS* f_{60}/f_{25} flux ratio is not an good indicator of the inclination, but of the relative strength of the host galaxy and nucleus emission. These studies (also see Cheng et al. 2002; Lumsden & Alexander 2001), instead, have shown that the presence of PBLs in Sy2s depends on the AGN luminosity: Sy2s with PBLs have higher luminosity, compared with Sy2s without PBLs. Explanations of the observational results include the following: (1) The contribution from the host galaxy or from a circumnuclear starburst would dilute the nuclear optical spectrum, making the detection of PBLs more difficult for Sy2s with lower luminosity (Alexander 2001; Gu et al. 2001). (2) Alternatively, Tran (2001, 2003; also see Yu & Hwang 2005) suggested that at least some of the Sy2s without PBLs are powered by starbursts rather than accretion onto a supermassive black hole; therefore, the BLRs simply do not exist. (3) More luminous sources tend to have a large scale height of the scattering region, thus increasing the visibility of PBLs (Lumsden & Alexander 2001). (4) Nicastro et al. (2003) have argued that at very low accretion rates (and therefore lower luminosities), the clouds of the BLRs would cease to exist, and the absence of PBLs in Sy2s is consistent with their low accretion rates. (5) In the case of low-luminosity nuclei, the adjacent bright sources can easily outshine the nuclear flux, and the N_{H} derived from the X-ray spectrum may be underestimated (e.g., Georgantopoulos & Zezas 2003). (6) The large-scale dusty environment (Panessa & Bassani 2002) or complex and variable obscuring material (Matt 2000; Risaliti 2002) may to some extent affect the appearance of PBLs in Sy2s. (7) Long-term large-amplitude variations in the nuclear activity could vary the PBL flux and thus the detectability of PBLs (Lumsden et al. 2004).

Meanwhile, it is worth to note that there is also weak evidence showing different absorption in the two types of Sy2s: Gu et al. (2001) found a slightly (but not statistically conclusive) lower N_{H} for PBL Sy2s, and Lumsden et al. (2004) found a considerably higher detection rate of scattered broad Hα in a small sample of Compton-thin Sy2s. Note that one must be cautious when comparing the fraction of PBL Sy2s between samples, since the luminosity might have played a major role. These evidences suggest that besides the AGN luminosity, the X-ray absorption column

TABLE 1

Optical and Hard X-Ray Data for Seyfert 2 Galaxies with and without PBLs

Name (1)	z (2)	PBL? (3)	References[a] (4)	$F_{\lambda 5007}$ (5)	$L_{[O\,III]}$ (6)	References (7)	$F_{2-10\,keV}$ (8)	log N_H (9)	EW(Fe) (10)	References (11)
Lumsden et al. (2001)'s Sample										
Mrk 334	0.022	N	1	2.0	42.34	17	<13	20.643	...	41
IRAS 00198−7926	0.0728	N	2	0.36	42.67	18	<0.1	>24	...	42
NGC 1068	0.0038	Y	3L	67.8	42.33	17	4.62	>25	1200 ± 500	43
NGC 1143	0.0291	N	2	0.48	41.97	2	...	...	...	...
IRAS 04259−0440	0.0155	N	2	1.3	41.85	2	...	...	...	...
IRAS 05189−2524	0.0426	Y	4A	1.3	42.74	2	4.3	22.756	30^{+50}_{-30}	2
NGC 4388	0.0084	Y	4A	4.51	41.85	17	7.62	23.43	440^{+90}_{-90}	43
IC 3639	0.0109	Y	2	2.9	41.89	19	0.08	>24.204	1500^{+1100}_{-1100}	44
MCG −3-34-64	0.0165	Y	4A	4.0	42.39	2	4.0	23.614	356^{+186}_{-143}	45
NGC 5135	0.0137	N	2, 5A	6.61	42.44	19	0.16	>23.954	1700^{+600}_{-800}	46
NGC 5194	0.0015	N	2, 6L	2.2	40.03	20	0.48	24.748	986^{+210}_{-210}	43
NGC 5256	0.0278	N	2, 6L	0.44	41.89	17	0.56	>25	575	42
Mrk 1361	0.0226	N	2	1.8	42.32	2	...	...	...	...
NGC 5929*	0.0083	Y	7K	1.53	41.40	2	1.35	22.629	...	47
NGC 5995	0.0252	Y	2	6.6	42.98	2	22	21.934	240^{+240}_{-160}	2
IRAS 19254−7245*	0.0617	Y	8E	1.26	43.06	21	0.23	>24	2000 ± 600	48
IC 5063	0.0114	Y	9A	1.26	41.56	22	12	23.342	80^{+42}_{-50}	38
NGC 7130	0.0162	N	2	6.0	42.55	19	0.16	>24	1800^{+700}_{-800}	49
NGC 7172	0.0087	N	2	0.04	39.83	23	22	22.95	40 ± 30	50
IC 5298	0.0273	N	2	1.7	42.46	2	...	...	...	...
NGC 7582	0.0053	N	2, 5A	3.69	41.36	19	4.0	23.95	521^{+139}_{-141}	51
NGC 7674	0.0289	Y	4A, 10L	1.93	42.57	17	0.7	>24	370^{+160}_{-170}	52
Tran (2001)'s Sample										
IRAS 00521−7054	0.0689	N	4A	0.36	42.62	4	<31.8	...	...	30
IRAS 01475−0740	0.0177	Y	6P	0.82	41.76	18	0.75	21.59	130 (<344)	50
IRAS 02581−1136	0.0299	Y	6L	0.07	41.16	17	...	...	...	...
IRAS 04385−0828	0.0151	Y	6LP	0.086	40.64	24	2.4	...	...	30
IRAS 05189−2524	0.0426	Y	4A	1.3	42.74	2	4.3	22.756	30^{+50}_{-30}	2
IRAS 15480−0344	0.03	Y	4A, 6P	5.03	43.02	18	0.37	>24.204	<2400	44
IRAS 22017+0319	0.0611	Y	4A, 6P	0.42	42.58	4	3.6	22.69	380^{+180}_{-160}	53
IC 5063	0.0114	Y	9A	1.26	41.56	22	12	23.342	80^{+42}_{-50}	38
MCG −3-34-64	0.0165	Y	4A	4.0	42.39	2	4.0	23.614	356^{+186}_{-143}	45
Mrk 348	0.0151	Y	10L	1.77	41.96	17	4.8	23.204	212^{+68}_{-72}	54
MCG −3-5-87	0.0317	Y	6P	0.37	41.93	24	...	...	...	...
Mrk 463E	0.051	Y	4A, 10L	1.25	42.89	17	1.46	23.51	340^{+70}_{-90}	55
NGC 424	0.0117	Y	11C	1.18	41.56	25	1.6	24.301	790	56
NGC 513	0.0195	Y	12L	0.16	41.14	24	...	...	...	...
NGC 1068	0.0038	Y	3L	67.8	42.33	17	4.62	>25	1200 ± 500	43
NGC 4388	0.0084	Y	4A	4.51	41.85	17	7.62	23.43	440^{+90}_{-90}	43
NGC 5506	0.0062	N	6	3.33	41.45	15	58	22.46	86^{+24}_{-10}	57
NGC 5995	0.0252	Y	2	6.6	42.98	2	22	21.934	240^{+240}_{-160}	2
NGC 6552	0.0265	Y	6P	1.6	42.41	24	0.43	23.85	1408^{+668}_{-883}	50
NGC 7674	0.0289	Y	4A, 10L	1.93	42.57	17	0.7	>24	370^{+160}_{-170}	52
NGC 7682	0.0171	Y	6P	0.87	41.76	26	<13	...	...	30
IC 3639	0.0109	Y	2	2.9	41.89	19	0.08	>24.204	1500^{+1100}_{-1100}	44
IRAS 00198−7926	0.0728	N	2	0.36	42.67	18	<0.1	>24	...	42
IRAS 03362−1642	0.0372	N	3L	0.13	41.62	18	...	...	...	...
IRAS 19254−7245*	0.0617	Y	8E	1.26	43.06	21	0.23	>24	2000 ± 600	48
NGC 5194	0.0015	N	2, 6L	2.2	40.03	20	0.48	24.748	986^{+210}_{-210}	43
NGC 5256	0.0278	N	2, 6L	0.44	41.89	17	0.56	>25	575	42
Mrk 573*	0.0173	Y	5S	1.77	42.08	17	0.12	>24	2800^{+1820}_{-1220}	50
NGC 34	0.0198	N	5A, 6P	7.68	42.83	27	0.23	>24	<321	50
NGC 1144	0.0289	N	5A, 6P	0.39	41.87	23, 27	<12	20.699	...	41
NGC 1241	0.0135	N	6P	0.91	41.57	23, 24	...	...	...	...
NGC 1320	0.0094	N	6L	0.57	41.05	28	<8.2	...	...	30
NGC 1386	0.0029	N	11	10.2	41.27	29	0.27	>24.342	1800^{+400}_{-300}	46
NGC 1667	0.0152	N	6L, 11	2.03	42.02	19	0.1	>24	600	52
NGC 3079	0.0038	N	6L	0.92	40.47	20	0.33	25	1480^{+500}_{-500}	43
NGC 3362	0.0276	N	6L	0.13	41.36	30	<12.6	...	...	30
NGC 3660	0.0123	N	6L	0.17	40.76	19, 31	2.22	20.26	...	47
NGC 3982	0.0037	N	6L, 11	0.66	40.3	6, 20	0.057	>24	6310^{+3500}_{-3170}	50

TABLE 1—*Continued*

Name (1)	z (2)	PBL? (3)	References[a] (4)	$F_{\lambda 5007}$ (5)	$L_{[\mathrm{O\,III}]}$ (6)	References (7)	$F_{2\text{–}10\ \mathrm{keV}}$ (8)	$\log N_{\mathrm{H}}$ (9)	EW(Fe) (10)	References (11)
Tran (2001)'s Sample										
NGC 4501	0.0076	N	6L	0.06	39.89	20	0.11	<21.03	...	43
NGC 4941	0.0037	N	11	4.57	41.14	29	0.66	23.653	1600^{+700}_{-900}	58
NGC 5135	0.0137	N	2, 5A	6.61	42.44	19	0.16	>23.954	1700^{+600}_{-800}	46
NGC 5283	0.0104	N	6L, 11	0.4	40.98	17	1.46	23.176	<220	44
NGC 5347*	0.0078	Y	7K	1.14	41.19	6	0.22	>24	1300 ± 500	59
NGC 5695	0.014	N	6L, 11	0.081	40.55	17	<0.01	...	...	30
NGC 5929*	0.0083	Y	7K	1.53	41.40	2	1.35	22.629	...	47
NGC 6890	0.0081	N	11	0.5	40.86	32	...	...	...	...
NGC 7172	0.0087	N	2	0.04	39.83	23	22	22.95	40 ± 30	50
NGC 7582	0.0053	N	2, 5A	3.69	41.36	19	4.0	23.95	521^{+139}_{-141}	51
UGC 6100	0.0295	N	6L	0.96	42.28	26	<11.4	...	...	30
Moran et al. (2000)'s Sample										
IC 3639	0.0109	Y	2	2.9	41.89	19	0.08	>24.204	1500^{+1100}_{-1100}	44
ESO 428-G014	0.0056	N	11	20.1	42.15	33	0.38	>25	1600 ± 500	59
MCG +1-27-020	0.0117	N	11	...	...	...	...	...	...	...
Mrk 3	0.0135	Y	10L	46.1	43.27	32	5.9	24.134	610^{+30}_{-50}	60
Mrk 1066	0.012	N	10L	5.14	42	32	0.23	>24	1120^{+850}_{-650}	50
Mrk 348	0.0151	Y	10L	1.77	41.96	17	4.8	23.204	212^{+68}_{-72}	54
NGC 424	0.0117	Y	11C	1.18	41.56	25	1.6	24.301	790	56
NGC 591	0.0152	Y	11K	1.78	41.97	32	0.2	>24.204	2200^{+700}_{-600}	44
NGC 788	0.0136	Y	13L	0.15	40.79	34	4.62	23.324	...	47
NGC 1068	0.0038	Y	3L	67.8	42.33	17	4.62	>25	1200 ± 500	43
NGC 1358	0.0134	N	11	0.18	40.86	32	0.86	23.6	...	61
NGC 1386	0.0029	N	11	10.2	41.27	29	0.27	>24.342	1800^{+400}_{-300}	46
NGC 1667	0.0152	N	6L, 11	2.03	42.02	19	0.1	>24	600	52
NGC 1685	0.0152	N	11	9.09	42.67	26	<2	...	...	30
NGC 2273	0.0061	Y	11K	1.64	41.13	35	0.69	>24.126	2200^{+400}_{-300}	46
NGC 3081	0.0079	Y	11K	1.95	41.43	19	1.3	23.819	610^{+390}_{-210}	38
NGC 3281	0.0115	N	11	1.0	41.47	36	2.9	24.197	1180^{+400}_{-361}	62
NGC 3982	0.0037	N	6L, 11	0.66	40.3	6, 20	0.057	>24	6310^{+3500}_{-3170}	50
NGC 4117	0.0031	N	11	...	...	...	<23.2	...	...	30
NGC 4388	0.0084	Y	4A	4.51	41.85	17	7.62	23.43	440^{+90}_{-90}	43
NGC 4507	0.0118	Y	11K	4.98	42.19	32	12.8	23.643	117	63
NGC 4941	0.0037	N	11	4.57	41.14	29	0.66	23.653	1600^{+700}_{-900}	58
NGC 5135	0.0137	N	2, 5A	6.61	42.44	19	0.16	>23.954	1700^{+600}_{-800}	46
NGC 5283	0.0104	N	6L, 11	0.4	40.98	17	1.46	23.176	<220	44
NGC 5728	0.0094	N	4A, 11	7.61	42.18	19	1.33	23.89	1100^{+320}_{-270}	50
NGC 5643	0.004	N	11	6.62	41.37	32	0.84	23.845	500	64
NGC 5347*	0.0078	Y	7K	1.14	41.19	6	0.22	>24	1300 ± 500	59
NGC 5695	0.014	N	6L, 11	0.081	40.55	17	<0.01	...	...	30
NGC 5929*	0.0083	Y	7K	1.53	41.40	2	1.35	22.629	...	47
NGC 6890	0.0081	N	11	0.5	40.86	32	...	...	...	...
NGC 7672	0.0134	N	10L	...	...	...	28.6	...	...	30
Young et al. (1996)'s Sample										
IRAS 00521−7054	0.0689	N	4A	0.36	42.62	4	<31.8	...	...	30
IRAS 04103−2838	0.118	N	4A	...	...	...	...	...	...	...
IRAS 04210+0400	0.046	N	4A	0.554	42.44	4	...	...	...	...
IRAS 04229−2528	0.044	N	4A	0.216	41.99	4	...	...	...	...
IRAS 04385−0828	0.0151	Y	6LP	0.086	40.64	24	2.4	...	...	30
IRAS 05189−2524	0.0426	Y	4A	1.3	42.74	2	4.3	22.756	30^{+50}_{-30}	2
IRAS 11058−1131	0.055	Y	4A	0.394	42.45	4	0.39	>24	900	53
MCG −3-34-64	0.0165	Y	4A	4.0	42.39	2	4.0	23.614	356^{+186}_{-143}	45
IRAS 08277−0242	0.041	N	4A	1.42	42.75	18	...	...	...	...
IRAS 13452−4155	0.039	N	4A	...	...	...	...	...	...	...
ESO 273-IG04	0.039	Y	4A	0.85	42.48	4	...	...	...	...
IRAS 15480−0344	0.03	Y	4A, 6P	5.03	43.02	18	0.37	>24.204	<2400	44
IRAS 20210+1121	0.056	N	4A	2.73	43.31	4	0.29	>25	1650	53
IRAS 20460+1925	0.181	Y	4A	0.112	43.02	4	1.5	22.398	260^{+145}_{-137}	38
IRAS 22017+0319	0.0611	Y	4A, 6P	0.42	42.58	4	3.6	22.69	380^{+180}_{-160}	53
IRAS 23128−5919	0.045	N	4A	0.101	41.68	4	0.13	22.681	...	65

TABLE 1—*Continued*

Name (1)	z (2)	PBL? (3)	References[a] (4)	$F_{\lambda 5007}$ (5)	$L_{[\mathrm{O\,III}]}$ (6)	References (7)	$F_{2\text{–}10\ \mathrm{keV}}$ (8)	$\log N_{\mathrm{H}}$ (9)	EW(Fe) (10)	References (11)
Young et al. (1996)'s Sample										
NGC 5506	0.0062	N	6	3.33	41.45	15	58	22.46	86^{+24}_{-10}	57
Mrk 463E	0.051	Y	4A, 10L	1.25	42.89	17	1.46	23.51	340^{+70}_{-90}	55
NGC 4388	0.0084	Y	4A	4.51	41.85	17	7.62	23.43	440^{+90}_{-90}	43
NGC 5252	0.023	Y	4A	0.921	42.05	4	10.7	22.461	44 ± 28	50
NGC 5728	0.0094	N	4A, 11	7.61	42.18	19	1.33	23.89	1100^{+320}_{-270}	50
NGC 7496	0.005	N	4A	0.3	40.22	4	<8	22.699	...	30
NGC 7674	0.0289	Y	4A, 10L	1.93	42.57	17	0.7	>24	370^{+160}_{-170}	52
Other Surveys										
Mrk 1210	0.0135	Y	14L	5.8	42.37	37	9.3	23.263	108^{+50}_{-65}	66
IRAS 18325−5926	0.0202	Y	15L	1.68	42.19	15	10	22.31	242	67
MCG −5-23-16	0.008	Y	15A	4.09	41.81	38	70	22.25	$35.2^{+9.6}_{-10}$	68
Circinus	0.0014	Y	16	19.1	40.92	39	14	24.633	2250^{+260}_{-300}	69
Mrk 477	0.038	Y	14L	12.4	43.62	17	1.2	>24	490^{+250}_{-200}	38
NGC 2992	0.0077	Y	15A	1.49	41.3	15	4.5	21.84	514 ± 190	38
NGC 7314	0.0047	Y	15A	17.7	42.41	38	41.2	22.02	147^{+128}_{-109}	51
NGC 6300	0.0037	N	15A	3.2	40.99	15	21.6	23.342	148^{+18}_{-18}	70
NGC 7212	0.027	Y	14L	3.2	42.73	32	0.69	>24.204	900^{+200}_{-300}	44
NGC 7590	0.0053	N	5A	0.168	40.02	19	1.2	<20.964	...	38
Was 49b	0.063	Y	14L	33.8	42.51	40	0.63	22.799	620 ± 250	54

NOTE.—The Sy2s marked with an asterisk (*) denote cases in which the PBL was detected in later spectropolarimetric observations.

[a] Letters denote references that used the following telescopes: C = CTIO (4 m), P = Palomar (5 m), K = Keck (10 m), L = Lick (3 m), S = Subaru (8.2 m), E = ESO (3.6 m), and A = AAT (3.9 m).

REFERENCES.—(1) Ruiz et al. 1994; (2) Lumsden et al. 2001; (3) Antonucci & Miller 1985; (4) Young et al. 1996; (5) Heisler et al. 1997; (6) Tran 2001; (7) Moran et al. 2001; (8) Pernechele et al. 2003; (9) Inglis et al. 1993; (10) Miller & Goodrich 1990; (11) Moran et al. 2000; (12) Tran 1995; (13) Kay & Moran 1998; (14) Tran et al. 1992; (15) Lumsden et al. 2004; (16) Alexander et al. 2000; (17) Dahari & De Robertis 1988; (18) de Grijp et al. 1992; (19) Storchi-Bergmann et al. 1995; (20) Ho et al. 1997; (21) Duc et al. 1997; (22) Colina et al. 1991; (23) Vaceli et al. 1997; (24) Tran 2003; (25) Murayama et al. 1998; (26) Cruz-González et al. 1994; (27) Veilleux et al. 1995; (28) De Robertis & Osterbrock 1986; (29) Storchi-Bergmann & Pastoriza 1989; (30) Polletta et al. 1996; (31) Kollatschny et al. 1983; (32) Mulchaey et al. 1994; (33) Acker et al. 1991; (34) Whittle et al. 1992; (35) Lonsdale et al. 1992; (36) Storchi-Bergmann et al. 1992; (37) Terlevich et al. 1991; (38) Bassani et al. 1999; (39) Oliva et al. 1994; (40) Moran et al. 1992; (41) Prieto et al. 2002; (42) Risaliti et al. 2000; (43) Cappi et al. 2006; (44) Guainazzi et al. 2005a; (45) Dadina & Cappi 2004; (46) Guainazzi et al. 2005b; (47) tartarus.gsfc.nasa.gov; (48) Braito et al. 2003; (49) Levenson et al. 2005; (50) this work; (51) Dewangan & Griffiths 2005; (52) Bianchi et al. 2005b; (53) Ueno et al. 2000; (54) Awaki et al. 2000; (55) Imanishi & Terashima 2004; (56) Matt et al. 2003; (57) Bianchi et al. 2003; (58) Maiolino et al. 1998; (59) Levenson et al. 2006; (60) Bianchi et al. 2005a; (61) Fraquelli et al. 2003; (62) Vignali & Comastri 2002; (63) Matt et al. 2004; (64) Guainazzi et al. 2004; (65) Franceschini et al. 2003; (66) Ohno et al. 2004; (67) Iwasawa et al. 2004; (68) Dewangan et al. 2003; (69) Smith & Wilson 2001; (70) Matsumoto et al. 2004.

density also plays a role in the visibility of PBLs in Sy2s. We point out that the role of the absorption (if applicable) could reveal itself in a luminous Sy2 sample in which the influence of luminosity on the visibility of PBLs is weak enough.

In this paper we revisit the issue of whether the nuclear obscuration in Seyfert 2 galaxies affects the visibility of PBLs by focusing on luminous Sy2s. The launch of the *Chandra X-Ray Observatory* in 1999 and of *XMM-Newton* in 2000 opened a new era of X-ray astronomy. New *Chandra* and *XMM-Newton* observations have significantly enlarged the sample of Sy2s for which both spectropolarimetric and X-ray observations are available, and have also provided more reliable X-ray measurements, thanks to their much higher spatial resolution and better sensitivity. In this paper, we present a large sample of Sy2s for which both spectropolarimetric and X-ray data are available to probe the nuclear obscuration for PBL and NPBL Sy2s. Our sample consists of 29 PBL Sy2s and 25 NPBL Sy2s. Among them, 8 *Chandra* and 30 *XMM-Newton* observations are available either from the literature or from an archive. Throughout this paper, we use the cosmological parameters $H_0 = 70$ km s^{-1} Mpc^{-1}, $\Omega_m = 0.27$, and $\Omega_\lambda = 0.73$.

2. SAMPLE SELECTION

We collect all Sy2s with spectropolarimetric observations from the literature (from 1985 to 2006; see Table 1). The spectropolarimetric data are mainly from several large surveys, including the infrared-selected sample of Heisler et al. (1997), the far-infrared flux- and luminosity-limited sample of Lumsden et al. (2001), the distance-limited sample of Moran et al. (2000, 2001), the heterogeneous optical- and mid-infrared–selected sample of Tran (2001), and the infrared color-selected sample of Young et al. (1996). We then exclude NGC 2992, NGC 5506, NGC 5252, NGC 7314, MCG −3-34-64, and Mrk 334[1] from discussion due to their intermediate classification (i.e., Sy1.8s, Sy1.9s) in NED. To avoid luminosity selection bias due to the redshift difference when comparing properties between the PBL and NPBL Sy2s, we confine our sample to $z < 0.06$. We collect [O III] λ5007 and X-ray data from the literature, and we present spectra analysis of archival *Chandra* and *XMM-Newton* data for eight sources in § 3. The result from the most recent observation is adopted when two or more observations exist. Note that in the table, there are eight upper limits in the hard X-ray flux due to X-ray nondetection in the hard band, and their X-ray absorption column densities in the literature were estimated either from soft-band X-ray data or from the strength of their X-ray emission relative to the optical band. We exclude these values of N_{H} from the following analysis. NGC 4117 is also

[1] Among the six sources, NGC 5506 and Mrk 334 do not show PBLs in the polarized spectra, and the other four do. Including these sources in our sample does not make a significant difference to our major results.

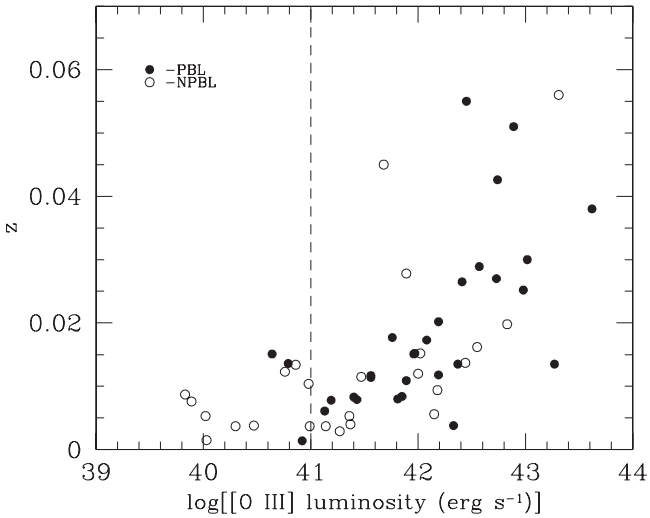

FIG. 1.—Redshift vs. [O III] λ5007 luminosity for two types of Sy2s in the sample. Solid circles stand for PBL Sy2s, and open circles represent NPBL Sy2s.

excluded, since its [O III] λ5007 flux is not available from the literature. This leaves a sample composed of 29[2] Sy2s with PBLs and 25 Sy2s without PBLs for which both the spectropolarimetric and X-ray data are available. Figure 1 shows the redshift against the luminosity of extinction-corrected [O III] λ5007 emission for PBL and NPBL Sy2s in the sample. As previous studies have shown, we clearly see higher luminosities for PBL Sy2s (with a confidence level of 99.7%), indicating that the nuclear activity plays a major role in the visibility of PBLs in Sy2s.

The optical and X-ray data are presented in Table 1. The table lists, in turn, the name of the galaxy, the redshift z as reported in NED, the spectropolarimetric properties, the corresponding references, the extinction-corrected flux of the [O III] λ5007 emission in units of 10^{-12} ergs s^{-1} cm^{-2}, the luminosity of the extinction-corrected [O III] λ5007 emission in units of ergs s^{-1}, the references for the [O III] λ5007 emission, the observed rest-frame hard X-ray (2–10 keV) flux in units of ergs s^{-1}, the X-ray absorption column density ($N_{\rm H}$) in units of cm^{-2}, the equivalent width (EW) of the fluorescence iron line in units of eV, and the references for the X-ray properties. The luminosity of the extinction-corrected [O III] λ5007 emission is given as $L_{[\rm O\,III]} = 4\pi D^2 F^{\rm cor}_{[\rm O\,III]}$, where $F^{\rm cor}_{[\rm O\,III]}$ is the extinction-corrected flux of [O III] λ5007 emission derived from the relation (Bassani et al. 1999)

$$F^{\rm cor}_{[\rm O\,III]} = F^{\rm obs}_{[\rm O\,III]} \left[\frac{(\rm H\alpha/H\beta)_{\rm obs}}{(\rm H\alpha/H\beta)_0}\right]^{2.94}.$$

We assume an intrinsic Balmer decrement of $(\rm H\alpha/H\beta)_0 = 3.0$.

[2] For one galaxy, IRAS 04385−0828, the value of $N_{\rm H}$ is unavailable, but we can get the reference to the hard X-ray flux from Polletta et al. (1996). When using the T ratio for analysis, the number of PBL Sy2s is 30.

3. X-RAY SPECTRAL ANALYSIS

In this section, we report the results of X-ray spectral fitting to archival *Chandra* and *XMM-Newton* spectra of eight Sy2s in the sample. The data were reduced using CIAO version 3.2.2 and XMMSAS version 6.5.0, respectively. The size of each source on the detector was estimated in order to determine appropriate source extraction regions, typically of $\sim$2″ radius (*Chandra*) or $\sim$30″ radius (*XMM-Newton*) for on-axis point sources. The background spectra were extracted from a source-free annulus around the source. The spectra of each galaxy were binned to a minimum of 1 count per bin, and we adopt the C-statistic (Cash 1979) for minimization. Spectral fits were performed using XSPEC version 11.2 in the 0.5–8 keV band. All the quoted errors indicate the 90% confidence range for one parameter of interest.

Each spectrum was initially fitted with a simple model consisting of a power law plus Galactic and intrinsic neutral absorption. In many cases this simple parameterization is not sufficient to model the whole 0.5–8 keV spectrum. Residuals often show a soft excess on top of the power law. The soft excess is fitted here as a scattered power-law component (with the same power-law slope but no intrinsic absorption). The possible presence of a narrow emission line centered at 6.4 keV originating from neutral iron has also been checked and is modeled with a single Gaussian line.

We note that in Compton-thick sources with $N_{\rm H} > 10^{24}$ cm^{-2}, the transmitted component is heavily suppressed below 10 keV, and the spectrum observed in the 2–10 keV band might be dominated by the reflection component (Matt et al. 2000). In this paper, NGC 34, NGC 3982, Mrk 573, and Mrk 1066 are classified as Compton-thick sources on the basis of their large Fe Kα EWs (>1 keV, except for NGC 34; see notes in the Appendix) and their small $F_{2\text{–}10\,\rm keV}/F_{[\rm O\,III]}$ ratios (<0.1; Maiolino et al. 1998; Bassani et al. 1999; Guainazzi et al. 2005b). For Compton-thick sources, we use a reflection model (the `pexrav` model in XSPEC; Magdziarz & Zdziarski 1995) for spectrum fitting.

TABLE 2
BEST-FIT PARAMETERS FOR THE X-RAY SPECTRAL ANALYSIS

Name (1)	Observatory (2)	Obs. Date (3)	$N_{\rm H}$ (4)	Γ (5)	Center Energy (6)	EW(Fe K) (7)	f_s (%) (8)	C/dof (9)	$F_{2\text{–}10\,\rm keV}$ (10)	T (11)
NGC 34	*XMM-Newton*	2002 Dec 22	>100	2.38 ± 0.1	6.4[a]	<321	...	362/448	0.23	0.03
NGC 3982	*XMM-Newton*	2004 Jun 15	>100	$3.74^{+1.8}_{-1.6}$	6.4[a]	6310^{+3500}_{-3170}	...	109/135	0.057	0.086
NGC 5728	*Chandra*	2003 Jun 27	78^{+15}_{-14}	2.73 ± 0.17	6.39 ± 0.03	1100^{+320}_{-270}	0.4 ± 0.03	299/300	1.33	0.17
NGC 6552	*XMM-Newton*	2002 Oct 18	71^{+40}_{-10}	$2.8^{+0.37}_{-0.13}$	6.4[a]	1408^{+668}_{-883}	$0.75^{+0.09}_{-0.22}$	121/166	0.43	0.27
NGC 7172	*XMM-Newton*	2002 Nov 18	8.7 ± 0.57	1.49 ± 0.13	6.4[a]	40 ± 30	0.54 ± 0.1	463/495	22	550
Mrk 573	*XMM-Newton*	2004 Jan 15	>100	$3.7^{+0.08}_{-0.10}$	6.4[a]	2800^{+1820}_{-1220}	...	394/399	0.12	0.07
IRAS 01475−0740	*XMM-Newton*	2004 Jan 21	$0.39^{+0.04}_{-0.02}$	2.06 ± 0.06	6.4[a]	130 (<344)	...	631/776	0.75	0.92
Mrk 1066	*Chandra*	2004 Jul 18	>100	$2.75^{+0.17}_{-0.07}$	$6.34^{+0.17}_{-0.06}$	1120^{+850}_{-650}	...	497/505	0.23	0.05

NOTES.—Col. (1): Galaxy name. Col. (2): Instrument. Col. (3): Observation date. Col. (4): Power-law photon index. Col. (5): Measured absorption column density, in units of 10^{22} cm^{-2}. Col. (6): Fe line energy, in units of keV. Col. (7): Fe line equivalent width, in units of eV. Col. (8): Scattering fraction of the soft component. Col. (9): C-statistic and number of degrees of freedom (dof). Col. (10): Fitted 2–10 keV flux, in units of 10^{-12} ergs s^{-1} cm^{-2}. Col. (11): Ratio of $F_{2\text{–}10\,\rm keV}$ to $F_{[\rm O\,III]}$.

[a] Fixed value.

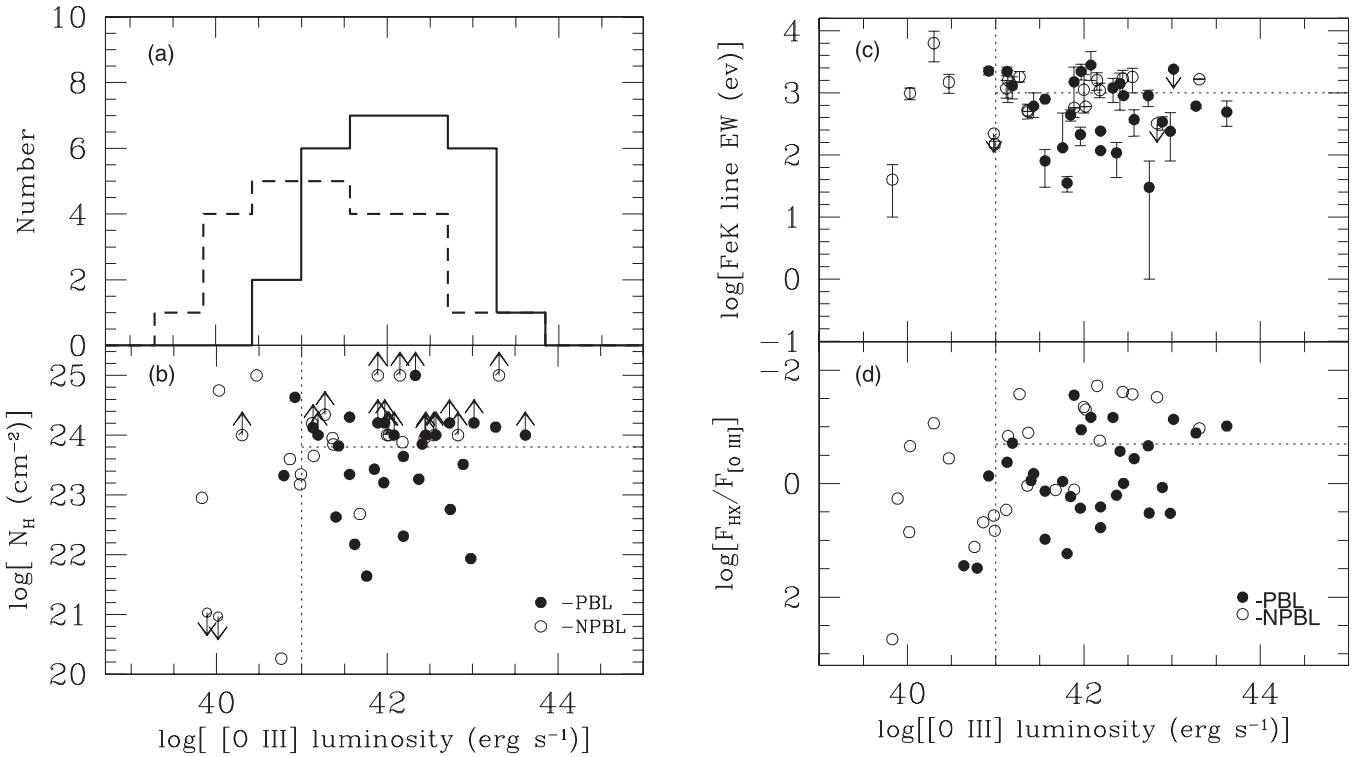

FIG. 2.—Different X-ray obscuration indicators vs. the [O III] luminosity for our sample. The bottom left panel plots the absorption column density N_H vs. the [O III] λ5007 luminosity for PBL and NPBL Sy2s. The distribution of the [O III] λ5007 luminosity for two types of Sy2s is presented in the top left panel (*solid line*, PBL Sy2s; *dashed line*, NPBL Sy2s). The right panel shows the plots of the Fe K line EW (*top*) and the *T* ratio (*bottom*) vs. the [O III] λ5007 luminosity.

Given the purpose of this work (to obtain a proper description of the spectra in terms of absorption, 2–10 keV flux, and Fe K line intensity), these simple parameterizations yield adequate fits to all the spectra presented here. The best-fit spectral parameters are listed in Table 2, and notes on individual objects are given in the Appendix.

4. DIFFERENT OBSCURATION IN TWO TYPES OF Sy2s

In Figure 2*b*, we plot the luminosity of the extinction-corrected [O III] λ5007 emission versus N_H. The separation is apparent for the two types of Sy2s. The diagram can be roughly divided into three regions with boundaries at $N_H = 10^{23.8}$ cm^{-2} and $L_{[O\,III]} = 10^{41}$ ergs s^{-1}. For the luminous Sy2s (with $L_{[O\,III]} > 10^{41}$ ergs s^{-1}), we can clearly see that most of the Sy2s with $N_H < 10^{23.8}$ cm^{-2} show PBLs (86%; 12 out of 14), while the fraction is much smaller for sources with heavier obscuration (54%; 15 out of 28). For the Sy2s with lower [O III] luminosity ($<10^{41}$ ergs s^{-1}), only a small fraction show PBLs (17%; 2 out of 12); due to the limited number of sources, we are not able to tell if the fraction of PBL sources depends on the X-ray absorption at lower luminosity.

In Figure 3 (*left*), we plot the N_H distributions for all Sy2s with and without PBLs. Since there are 11 censored data points (lower limits; *shaded areas*) among PBL Sy2s and 10 among NPBL Sy2s, we use the survival analysis methods ASURV (Feigelson & Nelson 1985) for statistical analysis. We find little difference (with a confidence level of 66.5% of the difference; see Table 3) in N_H between PBL and NPBL Sy2s, and the mean values of log N_H (in units of cm^{-2}) are 23.755 ± 0.19 and 23.852 ± 0.274, respectively (for NGC 4501 and NGC 7590, we adopt the N_H upper limits as the measured values, since ASURV could not deal with a case that contained both upper and lower limits). However, if we only consider the luminous Sy2s with $L_{[O\,III]} > 10^{41}$ ergs s^{-1}, a Kolmogorov-Smirnov (K-S) test shows that the probability for the two samples to be extracted from the same parent population is about 7.7%, and the mean values of log N_H are 23.739 ± 0.212 and 24.428 ± 0.192, respectively (Fig. 3, *right*). The results suggest that for luminous Sy2s in our sample, sources without PBLs show larger obscuration than those with PBLs, with a confidence level of 92.3%.

To further examine if obscuration plays a role in the detection/visibility of PBLs in Sy2s, we explore other potential measures of obscuration. By studying a large sample of Sy2s, Bassani et al. (1999) found that the thickness ("*T*") ratio $F_{2\text{–}10\,keV}/F_{[O\,III]}$ is a good indicator of nuclear obscuration. In particular, it is anticorrelated with both the column density N_H and the Fe Kα line EW, and these quantities can be used as probes of the obscuration to the center of the AGN. In Figures 2*c* and 2*d* we plot the Fe Kα line EW and the *T* ratio versus the luminosity of the extinction-corrected [O III] λ5007 emission. Similar patterns as those seen in Figure 2*b* are also obvious: that is, for luminous Sy2s, the NPBL sources tend to be more obscured. Figure 4 shows the *T* ratio distributions for all Sy2s (*left*) and for luminous objects only (*right*). A K-S test shows that the possibility for these two samples to be extracted from the same parent population is about 25%. The mean values of log *T* are −0.087 ± 0.145 and −0.342 ± 0.217 for Sy2s with and without PBLs, respectively. Similarly, the confidence level for the difference is much higher (at a level of 99.1%) for luminous Sy2s only. Turning to the Fe Kα line EW, K-S tests also confirm that for luminous Sy2s, the difference between the two samples is present (at the 95.3% level) with the available data. The mean values of log EW(Fe) are 2.626 ± 0.107 and 2.999 ± 0.066, respectively. After examining three independent indicators for obscuration, we conclude that for luminous Sy2s, sources without PBLs have higher obscurations than those with PBLs, confirming the suggestion that

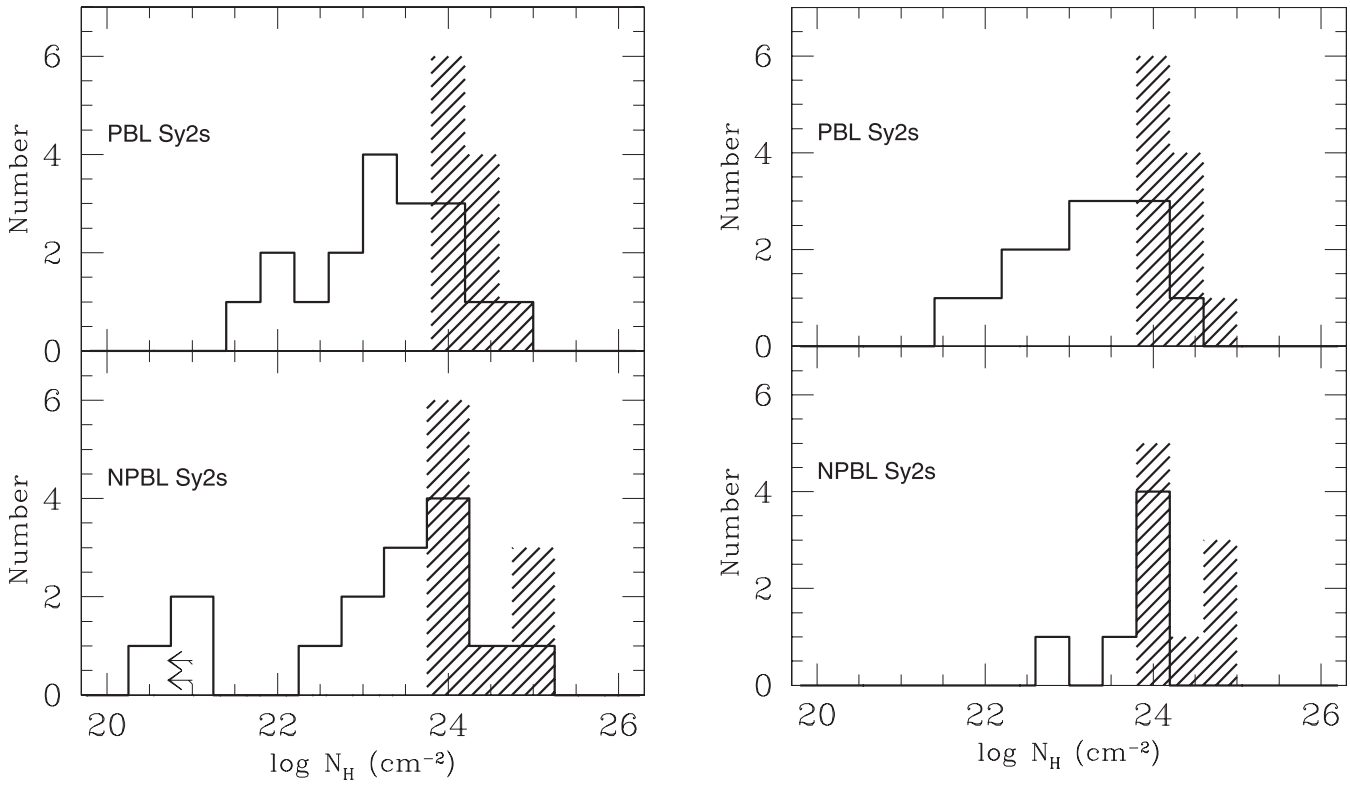

FIG. 3.—Distributions of N_H for all the Sy2s in our sample (*left*) and for luminous sources with $\log L_{[O\,III]} > 41$ ergs s^{-1} (*right*). Shaded areas denote lower limits. The arrows denote the upper limits of N_H.

the obscuration does play an important role in the detectability/visibility of PBLs. The results from the K-S tests and average values for N_H, the T ratio, and the Fe K line EW are summarized in Table 3.

5. DISCUSSION

It is clear that, as many previous studies have shown, PBL Sy2s have higher luminosities than NPBL Sy2s (see Figs. 1 and 2), indicating that the primary determinant of PBL visibility is the nuclear luminosity. In this paper, by focusing on luminous Sy2s, we find that the nuclear obscuration also plays an important role in the visibility of PBLs. For Sy2s with $L_{[O\,III]} > 10^{41}$ ergs s^{-1} in our sample, we find that NPBL Sy2s have a higher X-ray column density than PBL Sy2s at a significance level of 92.3%. When using the T ratio or the Fe K line EW as an indicator of nuclear obscuration, the confidence level of the difference in obscuration gets even higher (99.1% and 95.3%, respectively). Our results are consistent with those of Lumsden et al. (2004), who reported a higher detection rate of PBLs in Compton-thin Sy2s, but with a much higher confidence level. Consistent with previous studies, most (83%) of the less luminous Sy2s ($L_{[O\,III]} < 10^{41}$ ergs s^{-1}) do not show PBLs, the nature of which is still unclear (see § 1) and is beyond the scope of this paper. We also demonstrate that since most of the less luminous Sy2s do not show PBLs independent of absorption, adding them to the sample weakens the difference in obscuration found in the luminous sample. This explains why previous studies, which did not exclude less luminous sources, found no difference in absorption.

TABLE 3
SUMMARY OF THE STATISTICAL PROPERTIES OF Sy2s

Parameters	Sy2s with PBLs	Sy2s without PBLs	Note[a]	p_{null}[b] (%)
$\log T$	-0.087 ± 0.145	-0.342 ± 0.217	Total	25
	-0.201 ± 0.138	-0.87 ± 0.186	Luminous	0.9
$\log T$[c]	-0.093 ± 0.144	-0.436 ± 0.199	Total	13.5
	-0.203 ± 0.137	-0.899 ± 0.179	Luminous	0.68
log EW(Fe)	2.654 ± 0.107	2.85 ± 0.127	Total	18.6
	2.626 ± 0.107	2.999 ± 0.066	Luminous	4.67
$\log N_H$	23.755 ± 0.190	23.852 ± 0.274	Total	66.5
	23.739 ± 0.212	24.428 ± 0.192	Luminous	7.7
$\log L_{[O\,III]}$	42.099 ± 0.13	41.338 ± 0.188	Total	0.34
	42.198 ± 0.121	41.991 ± 0.157	Luminous	30.6
$\log z$	0.020 ± 0.003	0.017 ± 0.004	Luminous	29.4

[a] "Total" indicates all Sy2s with X-ray data in the sample. "Luminous" indicates Sy2s with $L_{[O\,III]} > 10^{41}$ ergs s^{-1} only.

[b] The possibility p_{null} represents the null hypothesis that the two distributions are drawn at random from the same parent population.

[c] Includes the eight hard X-ray upper limits stated in § 2. When there are censored data, we use Gehan's generalized Wilcoxon test with permutation variance (GGW test; one kind of ASURV test).

5.1. *Selection Effect?*

It is worth stressing whether the difference in the nuclear obscuration between the two types of Sy2s could be due to a possible observational and sample selection bias. We note that our sample is an amalgamation of different observations with diverse quality of spectropolarimetric data. We first examine whether the nondetections of PBLs in the sample are due to the weakness/lack of PBLs or due to the limited sensitivities of the spectropolarimetric data. Lumsden et al. (2001) showed that the signal-to-noise ratio (S/N) in their sample is sufficient for all but two of the NPBL Sy2s and attributed the nondetections to significantly weaker scattered flux. Tran (2003) pointed out that the distributions of [O III] flux, which is a good indicator of the strength of the Seyfert nucleus, are virtually the same between the two types of Sy2s in his sample, suggesting that the nondetections are not likely due to the

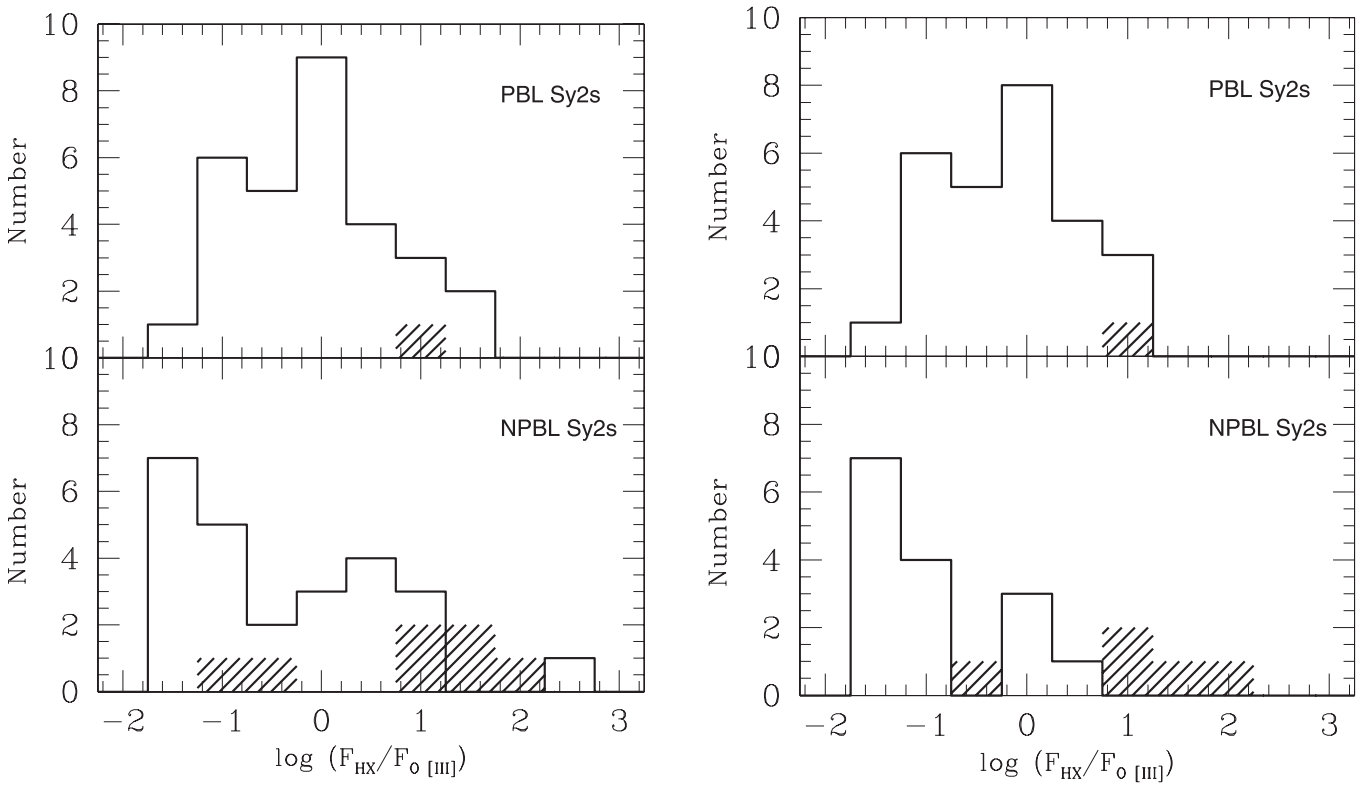

FIG. 4.—Distributions of the *T* ratio for all Sy2s (*left*) and for luminous Sy2s only (*right*) in our sample. Shaded areas denote the eight sources with only hard X-ray upper limits.

detection limit of the survey. The sensitivity of the sample of Moran et al. (2001) is found to be even better than that of the other samples mentioned above (Gu & Huang 2002). In Figure 5, we plot the *T* ratio versus the extinction-corrected [O III] flux for our composite sample. We can clearly see that for luminous sources (with $L_{[\mathrm{O\,III}]} > 10^{41}$ ergs s^{-1}) in our sample, there is no difference in the [O III] flux distributions between PBL and NPBL Sy2s. For comparison, sources with lower luminosities are also plotted, most of which are much weaker in [O III] flux. We conclude that most of the nondetections for our luminous sources are likely due to the weakness or lack of PBLs, but not due to the limited sensitivities of the spectropolarimetric data.

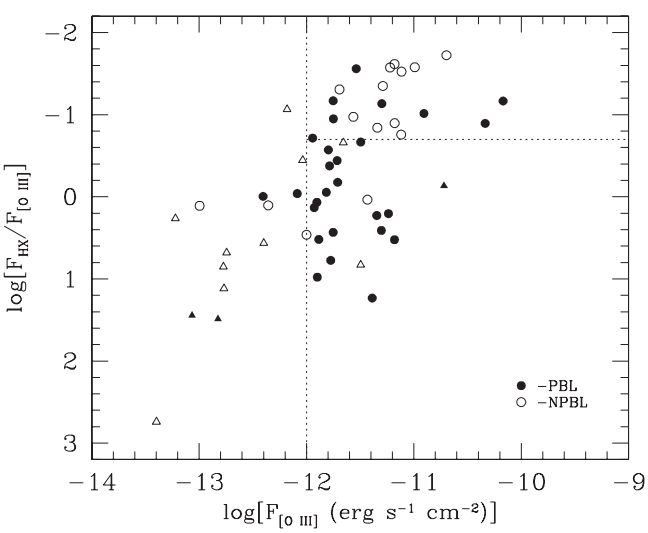

FIG. 5.—Plot of the *T* ratio vs. the extinction-corrected [O III] flux. Sources with luminosity $L_{[\mathrm{O\,III}]} < 10^{41}$ ergs s^{-1} are plotted as triangles.

We then verify whether our results are biased by combining samples with different selection criteria and survey depths into one single sample; that is, if some of the samples tend to select more obscured sources but with poor spectropolarimetric data, and/or some others tend to select less obscured sources but with better spectropolarimetric data. By plotting in Figure 6 the *T* ratio versus

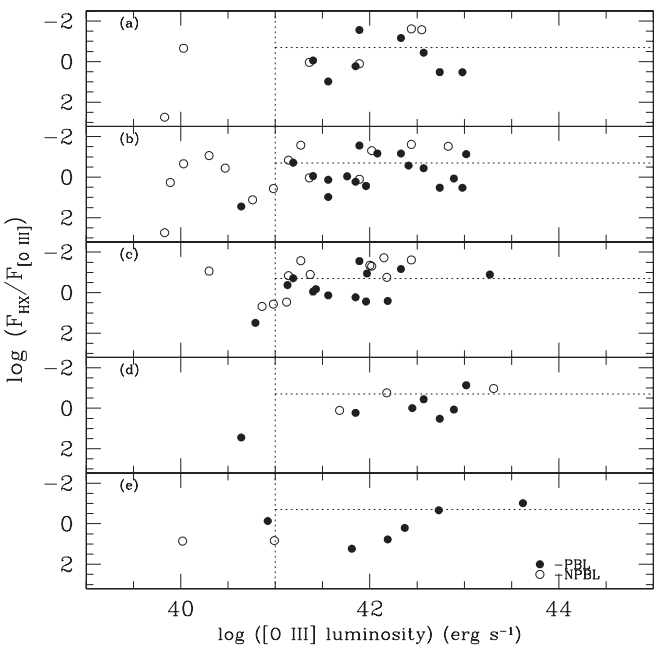

FIG. 6.—Plot of the *T* ratio vs. the [O III] λ5007 luminosity for different spectropolarimetric subsamples. (*a*) Lumsden et al. (2001)'s sample; (*b*) Tran (2001)'s sample; (*c*) Moran et al. (2000)'s sample; (*d*) Young et al. (1996)'s sample; (*e*) data from other surveys.

the [O III] luminosity for the sources in each subsample, we can see that this is not the case for our composite sample. We find that each subsample spans an obscuration range similar to that of the composite sample, and the differences in the obscuration between PBL and NPBL Sy2s are also visible in most of the subsamples.

We made an additional test to check whether the distributions of z and [O III] luminosity for our luminous sample were different (see Figs. 1 and 2*a*). Using ASURV, we get average values of $\langle z \rangle = 0.02 \pm 0.003$ and $\langle \log L_{[\mathrm{O\,III}]} \rangle = 42.198 \pm 0.121$ for PBL Sy2s, whereas we get $\langle z \rangle = 0.017 \pm 0.004$ and $\langle \log L_{[\mathrm{O\,III}]} \rangle = 41.991 \pm 0.157$ for NPBL Sy2s. The distributions of z and [O III] luminosity for luminous sources are similar at levels of $p_{\mathrm{null}} = 29.4\%$ and $p_{\mathrm{null}} = 30.6\%$, respectively. The similarity indicates that the difference in absorption could not be biased by different redshift or luminosity, both of which affect the visibility of PBLs. Also, the dilution effect, which is dependent on the redshift and luminosity, might bias the visibility of PBLs for less luminous Sy2s, but itself alone cannot explain the difference in the absorption between PBL and NPBL Sy2s. Actually, we note that the dilution effect for the visibility of PBLs is much weaker for our luminous sources. This can be seen from the fact that PBL Sy2s can be detected in most of our luminous Sy2s with smaller obscurations ($N_{\mathrm{H}} < 10^{23.8}$ cm^{-2}, or with a T ratio greater than $10^{-0.7}$). The dilution effect in X-rays (to the measurement of N_{H}) is also much weaker for luminous Sy2s. We conclude that there is no observational bias that can produce the difference in absorption between the two types of Sy2s in our sample, and that a physical link between the visibility of PBLs and nuclear obscuration is required.

5.2. *Physical Explanation of the Difference in Absorption*

The results presented here for luminous Sy2s can be interpreted within the context of the unified model for Seyfert galaxies, in agreement with the torus geometry portrayed by Heisler et al. (1997): the main electron scattering is confined to a conical region that is close to the thickness of the torus. More inclined Sy2s could have the broad-line scattering screen also obscured, thus making PBLs weaker or nondetectable. According to the unified model, more inclined sources are expected to have heavier obscuration, thus explaining the difference in obscuration between PBL and NPBL Sy2s.

Note that the high detection rate (86%) of PBLs in luminous Sy2s with $N_{\mathrm{H}} < 10^{23.8}$ cm^{-2} suggests that in most sources the Compton-thin X-ray–obscuring material cannot have a much larger scale than the scattering screen, supporting the torus scheme of the unified model. Furthermore, while extended obscuration from the host galaxy might explain the absence of PBLs in some sources (such as NGC 5506; see Lumsden et al. 2004), it could not be the major cause, or else we should have seen a large number of NPBL Sy2s among the luminous Sy2s with $N_{\mathrm{H}} < 10^{23.8}$ cm^{-2}. It is interesting to note that NGC 5506 is one of two intermediate Seyfert galaxies without PBLs detected (the other one is Mrk 334; see § 2), both with the BLR visible in the near-infrared. This suggests that extended obscuration from the host galaxy is also a plausible cause in the absence of PBLs in Mrk 334.

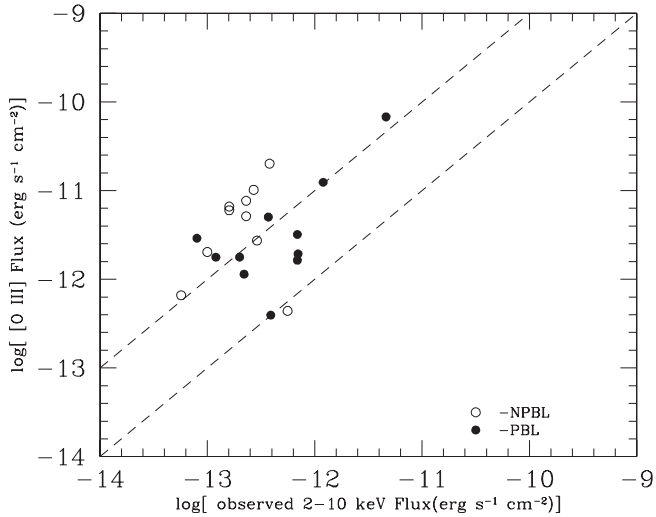

FIG. 7.—Observed [O III] flux (extinction-corrected) vs. X-ray (2–10 keV) flux for Compton-thick Sy2s (with $N_{\mathrm{H}} > 10^{24}$ cm^{-2}). The dashed lines represent $F_{[\mathrm{O\,III}]} = 10F_{2\text{–}10\,\mathrm{keV}}$ (*upper*) and $F_{[\mathrm{O\,III}]} = F_{2\text{–}10\,\mathrm{keV}}$ (*lower*).

We also note that when using the T ratio as an indicator of nuclear obscuration, the difference between the two types of Sy2s becomes more significant (see Fig. 2*d*). We point out that this is mainly because for Compton-thick sources, we can only give lower limits of $\sim 10^{24}$ cm^{-2} for N_{H}, but the T ratio is a continuous variable as long as the sources are detected in the X-ray band. Figure 7 shows the observed 2–10 keV X-ray flux against the extinction-corrected [O III] flux for Compton-thick Sy2s (with a lower limit of 10^{24} cm^{-2} of N_{H}, there are 11 PBL and 10 NPBL Sy2s). Interestingly, we find that although the lower limits of N_{H} are the same for the two types of Compton-thick Sy2s, NPBL Sy2s in the figure tend to be weaker in X-rays (with a confidence level of 97.6%). We note that the two types of Compton-thick Sy2s have similarly large Fe K line EWs (>1 keV), suggesting that the X-ray spectra in both types are reflection-dominated. In this case, the smaller T ratio in NPBL Sy2s can also be explained by higher inclination: sources viewed at higher inclination could have a large fraction of the inner surface of the torus, where the reflection component is produced, blocked from our line of sight, and thus expect weaker X-ray emission.

This work was supported by the Chinese NSF through NSF10473009/NSF10533050, and by the CAS "Bai Ren" project at the University of Science and Technology of China. The work in this paper has made use of NASA's Astrophysics Data System Abstract Service and the NASA/IPAC Extragalactic Database (NED), which is operated by the Jet Propulsion Laboratory, California Institute of Technology, under contract with NASA. This study has also made use of the HEASARC online data archive services, supported by NASA Goddard Space Flight Center.

APPENDIX

NOTES ON INDIVIDUAL OBJECTS

In this section, we present brief discussions for the X-ray data of three sources in the sample. All errors quoted are at the 90% level of confidence.

NGC 34.—We model the *XMM-Newton* 0.5–8.0 keV spectrum of this source with the `pexrav` model (C/dof = 362/448) in terms of its low T ratio of 0.03 (<0.1). However, the Fe K line is marginally detected, with an upper limit EW of 321 eV. We then fit the spectrum with an absorbed power-law model, which gives $\Gamma = 1.68^{+0.11}_{-0.17}$ but no intrinsic absorption, plus a Fe K line with EW = 386 (<1047) eV.

The model yields a worse fit, with $C/\mathrm{dof} = 389/448$. We note that the steep-spectrum slope may attribute to the host galaxy thermal emission in the soft X-ray band. From the lower T ratio of 0.03 (<0.1) and the better C-statistic of the `pexrav` model, we consider the galaxy as Compton-thick and give a lower limit of 10^{24} cm^{-2} to $N_{\rm H}$.

NGC 5728.—The *Chandra* 0.5–8 keV spectrum is parameterized here with an absorbed power law ($\Gamma = 2.73 \pm 0.17$, $N_{\rm H} = 7.8^{+1.5}_{-1.4} \times 10^{23}$ cm^2) plus a 0.4% scattered component. The Fe K line is detected at 6.4 keV, with EW $= 1100^{+320}_{-270}$ eV. For the lower T ratio and the large Fe line EW, we then fit the spectrum of this galaxy with the `pexrav` model plus a Gaussian line. However, the fitting is unacceptable ($C/\mathrm{dof} = 710/300$). Thus, we do not regard this source as a Compton-thick one in this paper. We note that considering it as Compton-thick does not affect our results as presented here.

NGC 6552.—We fit the *XMM-Newton* 0.5–8 keV spectrum of this source with an absorbed power law ($\Gamma = 2.8^{+0.37}_{-0.13}$) with a 0.75% scattered component. The best fit ($C/\mathrm{dof} = 121/166$) gives $N_{\rm H} = 7.1^{+4.0}_{-1.0} \times 10^{23}$ cm^2. The Fe K line is detected at 6.4 keV, with EW $= 1408^{+668}_{-883}$ eV. However, the `pexrav` model can also give an acceptable fitting of the spectrum, with $\Gamma = 2.86^{+0.34}_{-0.47}$ and a Fe K line EW $= 4990^{+3910}_{-2390}$ ($C/\mathrm{dof} = 128/166$). The fitted 2–10 keV flux is 2.32×10^{-13} ergs s^{-1} cm^{-2}. We adopt the absorbed power-law model for the spectrum fitting in the paper in terms of the better C-statistic. We note that the consideration of this source as Compton-thick does not affect our results as presented in this paper.

REFERENCES

Acker, A., Stenholm, B., & Veron, P. 1991, A&AS, 87, 499
Alexander, D. M. 2001, MNRAS, 320, L15
Alexander, D. M., Heisler, C. A., Young, S., Lumsden, S. L., Hough, J. H., & Bailey, J. A. 2000, MNRAS, 313, 815
Antonucci, R. 1993, ARA&A, 31, 473
Antonucci, R., & Miller, J. S. 1985, ApJ, 297, 621
Awaki, H., Ueno, S., Taniguchi, Y., & Weaver, K. A. 2000, ApJ, 542, 175
Bassani, L., Dadina, M., Maiolino, R., Salvati, M., Risaliti, G., della Ceca, R., Matt, G., & Zamorani, G. 1999, ApJS, 121, 473
Bianchi, S., Balestra, I., Matt, G., Guainazzi, M., & Perola, G. C. 2003, A&A, 402, 141
Bianchi, S., Guainaazi, M., Matt, G., Chiaberge, M., Iwasawa, K., Fiore, F., & Maiolino, R. 2005a, A&A, 442, 185
Bianchi, S., Miniutti, G., Fabian, A., & Iwasawa, K. 2005b, MNRAS, 360, 380
Braito, V., et al. 2003, A&A, 398, 107
Cappi, M., et al. 2006, A&A, 446, 459
Cash, W. 1979, ApJ, 228, 939
Cheng, L.-P., Zhao, Y.-H., & Wei, J.-Y. 2002, Chinese J. Astron. Astrophys., 2, 408
Colina, L., Sparks, W. B., & Macchetto, F. 1991, ApJ, 370, 102
Cruz-González, I., Carrasco, L., Serrano, A., Guichard, J., Dultzin-Hacyan, D., & Bisiacchi, G. F. 1994, ApJS, 94, 47
Dadina, M., & Cappi, M. 2004, A&A, 413, 921
Dahari, O., & De Robertis, M. M. 1988, ApJS, 67, 249
de Grijp, M. H. K., Keel, W. C., Miley, G. K., & Lub, J. 1992, A&AS, 96, 389
De Robertis, M. M., & Osterbrock, D. E. 1986, ApJ, 301, 98
Dewangan, G. C., & Griffiths, R. E. 2005, ApJ, 625, L31
Dewangan, G. C., Griffiths, R. E., & Schurch, N. J. 2003, ApJ, 592, 52
Duc, P. A., Mirabel, I. F., & Maza, J. 1997, A&AS, 124, 533
Feigelson, E. D., & Nelson, P. I. 1985, ApJ, 293, 192
Franceschini, A., et al. 2003, MNRAS, 343, 1181
Fraquelli, H. A., Storchi-Bergmann, T., & Levenson, N. A. 2003, MNRAS, 341, 449
Georgantopoulos, I., & Zezas, A. 2003, ApJ, 594, 704
Gu, Q., & Huang, J. 2002, ApJ, 579, 205
Gu, Q., Maiolino, R., & Dultzin-Hacyan, D. 2001, A&A, 366, 765
Guainazzi, M., Fabian, A. C., Iwasawa, K., Matt, G., & Fiore, F. 2005a, MNRAS, 356, 295
Guainazzi, M., Matt, G., & Perola, G. C. 2005b, A&A, 444, 119
Guainazzi, M., Rodriguez-Pascual, P., Fabian, A. C., Iwasawa, K., & Matt, G. 2004, MNRAS, 355, 297
Heisler, C. A., Lumsden, S. L., & Bailey, J. A. 1997, Nature, 385, 700
Ho, L., Filippenko, V., & Sargent, W. L. W. 1997, ApJS, 112, 315
Imanishi, M., & Terashima, Y. 2004, AJ, 127, 758
Inglis, M. D., Brindle, C., Hough, J. H., Young, S., Axon, D. J., Bailey, J. A., & Ward, M. J. 1993, MNRAS, 263, 895
Iwasawa, K., Lee, J. C., Young, A. J., Reynolds, C. S., & Fabian, A. C. 2004, MNRAS, 347, 411
Kay, L. E., & Moran, E. C. 1998, PASP, 110, 1003
Kollatschny, W., Biermann, P., Fricke, K. J., Huchtmeier, W., & Witzel, A. 1983, A&A, 119, 80
Levenson, N. A., Heckman, T. M., Krolik, J. H., Weaver, K. A., & Życki, P. T. 2006, ApJ, 648, 111
Levenson, N. A., Weaver, K. A., Heckman, T. M., Awaki, H., & Terashima, Y. 2005, ApJ, 618, 167
Lonsdale, C. J., Lonsdale, C. J., & Smith, H. E. 1992, ApJ, 391, 629
Lumsden, S. L., & Alexander, D. M. 2001, MNRAS, 328, L32
Lumsden, S. L., Alexander, D. M., & Hough, J. H. 2004, MNRAS, 348, 1451
Lumsden, S. L., Heisler, C. A., Bailey, J. A., Hough, J. H., & Young, S. 2001, MNRAS, 327, 459
Magdziarz, P., & Zdziarski, A. A. 1995, MNRAS, 273, 837
Maiolino, R., Salvati, M., Bassani, L., Dadina, M., della Ceca, R., Matt, G., Risaliti, G., & Zamorani, G. 1998, A&A, 338, 781
Matsumoto, C., Nava, A., Maddox, L. A., Leighly, K. M., Grupe, D., Awaki, H., & Ueno, S. 2004, ApJ, 617, 930
Matt, G. 2000, A&A, 355, L31
Matt, G., Bianchi, S., D'Ammando, F., & Martocchia, A. 2004, A&A, 421, 473
Matt, G., Bianchi, S., Guainazzi, M., Brandt, W. N., Fabian, A. C., Iwasawa, K., & Perola, G. C. 2003, A&A, 399, 519
Matt, G., Fabian, A. C., Guainazzi, M., Iwasawa, K., Bassani, L., & Malaguti, G. 2000, MNRAS, 318, 173
Miller, J. S., & Goodrich, R. W. 1990, ApJ, 355, 456
Moran, E. C., Barth, A. J., Kay, L. E., & Filippenko, A. V. 2000, ApJ, 540, L73
Moran, E. C., Halpern, J. P., Bothun, G. D., & Becker, R. H. 1992, AJ, 104, 990
Moran, E. C., Kay, L. E., Davis, M., Filippenko, A. V., & Barth, A. J. 2001, ApJ, 556, L75
Mulchaey, J., Koratkar, A., Ward, M. J., Wilson, A. S., Whittle, M., Antonucci, R. R. J., Kinney, A. L., & Hurt, T. 1994, ApJ, 436, 586
Murayama, T., Taniguchi, Y., & Iwasawa, K. 1998, AJ, 115, 460
Nicastro, F., Martocchia, A., & Matt, G. 2003, ApJ, 589, L13
Ohno, M., Fukazawa, Y., & Iyomoto, N. 2004, PASJ, 56, 425
Oliva, E., Salvati, M., Moorwood, A. F. M., & Marconi, A. 1994, A&A, 288, 457
Panessa, F., & Bassani, L. 2002, A&A, 394, 435
Pernechele, C., Berta, S., Marconi, A., Bonoli, C., Bressan, A., Franceschini, A., Fritz, J., & Giro, E. 2003, MNRAS, 338, L13
Polletta, M., Bassani, L., Malaguti, G., Palumbo, G. G. C., & Caroli, E. 1996, ApJS, 106, 399
Prieto, M. A., Pérez Garcia, A. M., & Rodriguez Espinosa, J. M. 2002, MNRAS, 329, 309
Risaliti, G. 2002, A&A, 386, 379
Risaliti, G., Gilli, R., Maiolino, R., & Salvati, M. 2000, A&A, 357, 13
Ruiz, M., Rieke, G. H., & Schmidt, G. D. 1994, ApJ, 423, 608
Smith, D. A., & Wilson, A. S. 2001, ApJ, 557, 180
Storchi-Bergmann, T., Kinney, A. L., & Challis, P. 1995, ApJS, 98, 103
Storchi-Bergmann, T., & Pastoriza, M. G. 1989, ApJ, 347, 195
Storchi-Bergmann, T., Wilson, A. S., & Baldwin, J. A. 1992, ApJ, 396, 45
Terlevich, R., Melnick, J., Masegosa, J., Moles, M., & Copetti, M. 1991, A&AS, 91, 285
Tran, H. D. 1995, ApJ, 440, 565
———. 2001, ApJ, 554, L19
———. 2003, ApJ, 583, 632
Tran, H. D., Miller, J. S., & Kay, L. E. 1992, ApJ, 397, 452
Turner, T. J., George, I. M., Nandra, K., & Mushotzky, R. F. 1997, ApJ, 488, 164
Ueno, S., Ward, M. J., O'Brien, P. T., Stirpe, G. M., & Matt, G. 2000, Adv. Space Res., 25, 823
Vaceli, M. S., Viegas, S. M., Gruenwald, R., & de Souza, R. E. 1997, AJ, 114, 1345
Veilleux, S., Goodrich, R. W., & Hill, G. J. 1997, ApJ, 477, 631
Veilleux, S., Kim, D. C., Sanders, D., Mazzarella, J. M., & Soifer, B. T. 1995, ApJS, 98, 171
Vignali, C., & Comastri, A. 2002, A&A, 381, 834
Whittle, M. 1992, ApJS, 79, 49
Young, S., Hough, J. H., Efstathiou, A., Wills, B. J., Bailey, J. A., Ward, M. J., & Axon, D. J. 1996, MNRAS, 281, 1206
Yu, P., & Hwang, C. 2005, ApJ, 631, 720